

# Compensation for the Response Function of Medium Energy Collimator in $^{67}\text{Ga}$ Planar and SPECT Imaging

C. Tocharoenchai<sup>1</sup>, B.M.W. Tsui<sup>1,2</sup>, D.P. Lewis<sup>3</sup>, E.C. Frey<sup>1,2</sup> and X. Zhao<sup>1</sup>

1. Department of Biomedical Engineering

2. Department of Radiology, University of North Carolina at Chapel Hill, NC

3. Division of Medical Physics, The Nathan Kline Institute for Psychiatric Research, NY

**T**he purpose of this study is to improve  $^{67}\text{Ga}$  planar and SPECT images by compensating for the response function of a medium energy (ME) collimator. The point response functions (PRFs) of a GE ME collimator for the 93, 185 and 300 keV photons of  $^{67}\text{Ga}$  at 5, 10, 15 and 20 cm from the collimator face were experimentally determined. For small pixel sizes, the PRFs at all source distances showed hole-pattern artifact. Images from the higher energy photopeaks showed increased penetration fractions resulting in long tails in the PRFs. For a specified source distance, a Butterworth filter can be designed to eliminate the collimator hole-pattern with minimal degradation of the spatial resolution. Compensation for the distance-dependent collimator-detector response was accomplished using iterative reconstruction methods. To evaluate the compensation methods, planar images and SPECT projection data were acquired from a phantom consisting of 3 hot spheres with diameters of 1, 1.3 and 1.6 cm inside a cylindrical phantom. The iterative reconstruction-based compensation method with appropriate filtering resulted in improved image resolution and contrast and fewer image artifacts as compared to filtered backprojection reconstruction without compensations. We conclude that the degradation caused by ME collimator in  $^{67}\text{Ga}$  imaging can be effectively compensated for using these techniques for improved image quality.

## I. INTRODUCTION

Gallium-67 citrate is a commonly used radiopharmaceutical for demonstrating primary and metastatic sites of a large variety of tumors. However, specially designed medium energy (ME) collimator is used and the quality of  $^{67}\text{Ga}$  images is often poor for two main reasons. First,  $^{67}\text{Ga}$  emits photons with several energies, including high energy photons that degrade the image quality due to septal penetration and

scatter in the collimator. Second, the thick septa and often long holes used in ME collimators tends to reduce the detection efficiency and generates hole-pattern artifact in the image. One potential way to improve the image quality is to compensate for the collimator-detector response degradation. Leichner et al.<sup>(1)</sup> showed the feasibility of SPECT imaging of 511 keV photons and using Butterworth filter with order 16 and cutoff frequency larger than

0.31 pixels<sup>-1</sup> caused no change in FWHM or FWTM. The hole-pattern was almost eliminated after filtering. Iterative reconstruction methods are a promising method for accomplishing this because they allow one to model the distance-dependent collimator-detector response function (CDRF), attenuation and scatter. Zeng et al.<sup>(2,3)</sup> demonstrated that the iterative reconstruction algorithm with CDRF compensation showed improvement in spatial resolution over the filtered backprojection (FBP) and the iterative reconstruction algorithms without CDRF compensation. The Ordered Subset Expectation Maximization (OS-EM) iterative algorithm<sup>(4,5)</sup> has been found to be especially useful due to its speed of convergence and favorable noise properties.

## II. EXPERIMENTAL DESIGN AND METHODS

### A. Determination of the Total Point Response Function

A GE dual-camera MAXXUS SPECT system equipped with a ME collimator designed for  $^{67}\text{Ga}$  imaging was used in this study. The collimator has hexagonal holes with a flat-to-flat size of 3.4 mm, septal thickness of 1.4 mm and hole length of 42 mm. In order to incorporate CDRF compensation, we experimentally determined the PRFs of the GE ME collimator. A  $^{67}\text{Ga}$  point source was placed at 5, 10, 15 and 20 cm from the face of the ME collimator. Planar images of the point source were acquired at each position using three 20% energy windows centered over each of the three main photopeaks: 93, 185 and 300 keV<sup>(6)</sup>. The planar images were acquired in 512x512 matrices with 1 mm x 1 mm pixels.

### B. Planar Imaging of Phantom

A water-filled cylindrical phantom consisting of 3 hollow spheres was used in the phantom study. The inner diameter of the cylindrical phantom was 21.6 cm and the inner diameters of the hollow spheres were 0.84, 1.14 and 1.54 cm. They were filled with  $^{67}\text{Ga}$  in concentrations of 129  $\mu\text{Ci/ml}$ , 218  $\mu\text{Ci/ml}$  and 297  $\mu\text{Ci/ml}$ , respectively. The phantom was placed with its central axis at about 13 cm from the collimator. Planar images of the phantom were acquired in 256x256 matrices (2mm x 2mm pixels) and with the same system and imaging protocols as used for the  $^{67}\text{Ga}$  point source.

### C. Filter Design and Data Processing

In this study, the CDRF consists of the geometric component of the ME collimator and the intrinsic resolution of the detector. A filter was designed based on PRFs of the collimator. The total PRF of a ME collimator ( $prf_i(\vec{r})$ ) is given by

..(1)

where

- ≡ a position vector in the reconstructed image plane,
- ≡ an intrinsic resolution function of the detector,
- ≡ an aperture function of the collimator hole (typically hexagonal),
- ≡ a delta function array representing the positions of the centers of the collimator hole (typically a hexagonal closed packed array),

- ≡ the average point response function of the collimator that includes its geometric, penetration and scatter components,
- ⊗ ≡ convolution operator,
- ≡ multiplication operator.

Equation (1) demonstrates the components that contribute to the total PRF of a ME collimator and their relationship. It is useful in the design of an appropriate filter to process the images obtained using the collimator.

To design a filter that will reduce the collimator hole-pattern in planar images with negligible loss of spatial resolution, we used the total PRF of the GE ME collimator at 10 cm for the 185 keV photons from  $^{67}\text{Ga}$ . The PRF is shown in Figure 1(a) and horizontal and vertical profiles through its center are shown in Figure 1(b) and (c), respectively. The overall shape of the PRF

shown in Figure 1(a) is due to the point response function of a single collimator hole, i.e., in Equation (1). The hole-pattern and the shape of each of the hexagonal hole are described by and in Equation (1), respectively.

The Fourier transform (FT) of PRF, i.e., the transfer function (TF), was calculated and is shown in Figure 2(a). From Equation (1), the FT of total response function of a single hole, i.e., the FT of the , contributes to the central part of the TF and the overall shape of the TF is spread out due to the FT of in Equation (1).

To design a filter that essentially eliminates the hole-pattern with little loss of spatial resolution, a filter is needed that preserves the central peak of the TF, which largely determines the spatial resolution. At the same time, the filter must attenuate the side lobes that contribute to the hole-pattern<sup>(1)</sup>.

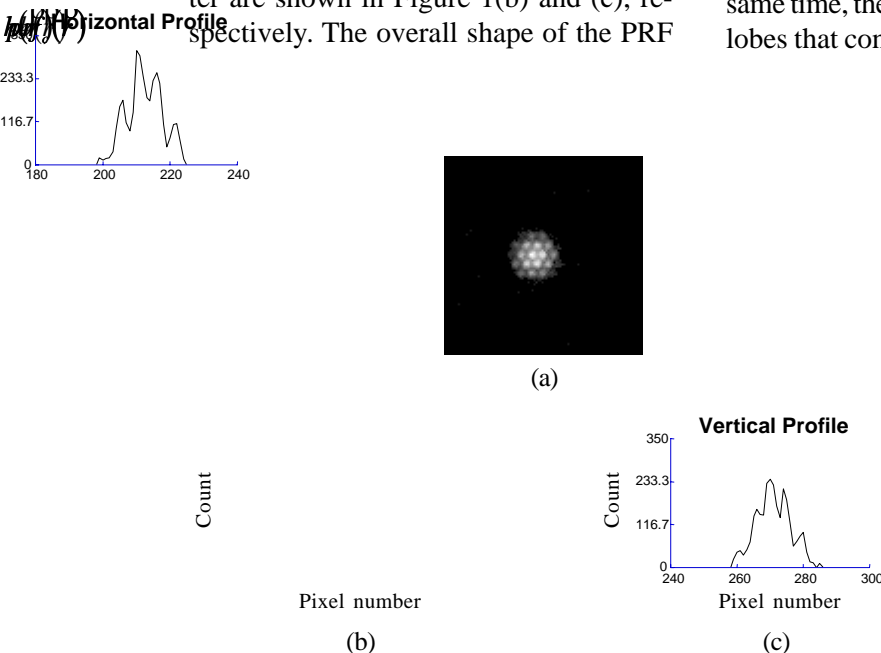


**Fig. 1** (a) The image of a  $^{67}\text{Ga}$  point source at 10 cm for the 185 keV photon at 20% energy window and (b) horizontal and (c) vertical profiles through the center of the image in (a).

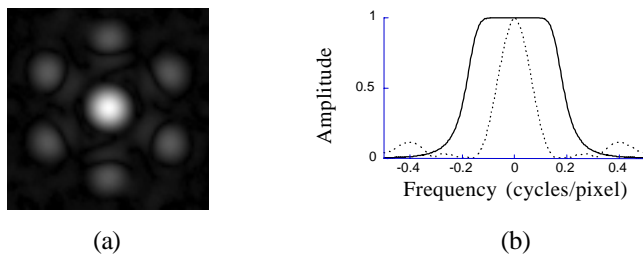


**Fig. 2** (a) The magnitude of the Fourier transform of the  $^{67}\text{Ga}$  point source image shown in Figure 1(a). (b) Vertical profile (...) through the center of (a) and a Butterworth filter (—) with order 5 and cutoff frequency 0.2 cycles/pixel.

Figure 2(b) shows an example of a Butterworth filter with order 5 and cutoff frequency at 0.2 cycles/pixel that accomplishes these goals.

#### D. SPECT Imaging of Phantom

Two hundred and fifty-six projection images of the cylindrical phantom were acquired over  $360^\circ$  with a 20 cm radius-of-rotation. Three 20% energy windows centered at the three  $^{67}\text{Ga}$  photopeaks described above were used. The projection images were acquired in  $128 \times 128$  matrices with 4 mm x 4 mm pixels. Another projection data set was obtained by collapsing the original  $128 \times 128$  image matrices into  $64 \times 64$  matrices. The projection data sets were reconstructed using FBP algorithm without any compensation. Two and five iterations of the OS-EM with and without CDRF compensation were also used in image reconstructions. The CDRF was calculated as a function of source distance<sup>(7)</sup> and then incorporated in the OS-EM iterative reconstruction algorithm. For each projection angle, rotation of the reconstructed image sampling grid was performed using bilinear interpolation, so that the rows were parallel to the detector face<sup>(8)</sup>. The pixel values in each row were then convolved with CDRF at the source distance. The resulting rows were then col-

lapsed to form the projection image for the current projection angle. Backprojection was performed using a similar algorithm.

### III. RESULTS

#### A. Total Point Response Function

The total PRF images of  $^{67}\text{Ga}$  acquired using the GE ME collimator and at 20% energy windows of the 185 keV photons at various distances are shown in Figure 3. The images demonstrate the change in the total PRF as a function of a source dis-

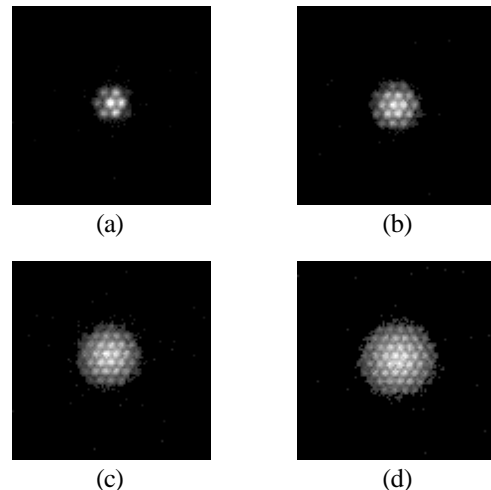


**Fig. 3** Images from the 185 keV energy window for a  $^{67}\text{Ga}$  point source placed at (a) 5 cm, (b) 10 cm, (c) 15 cm and (d) 20 cm from the collimator face.

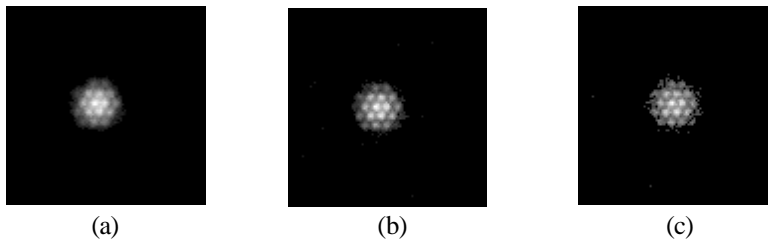


**Fig. 4** Images of a  $^{67}\text{Ga}$  point source placed at 10 cm from the collimator face for the (a) 93 keV, (b) 185 keV and (c) 300 keV photon energy windows.

tance. The PRFs images at 10 cm from the collimator face at the three main energies are shown in Figure 4. The hole-pattern is clearly demonstrated at all distances and different photon energies of  $^{67}\text{Ga}$  for the ME collimator.

### **B. Planar Images of phantom**

A sample planar image of the phantom with the 3 hot spheres is shown in Figure 5(a). It demonstrates the hole-pattern in the unprocessed images. A Butterworth filter of order 5 and cutoff frequency 0.1 cycles/

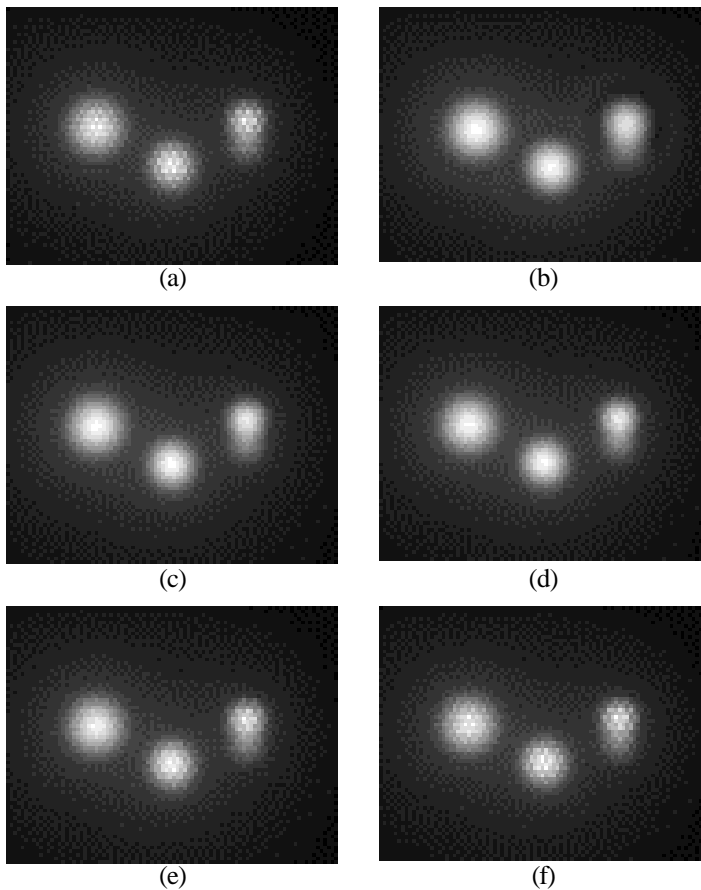


**Fig. 5** (a) An unfiltered planar image of the phantom acquired at 20% energy window of 185 keV photon. The processed images using Butterworth filter with order 5 and cutoff frequencies (b) 0.1, (c) 0.2, (d) 0.3, (e) 0.4 and (f) 0.5 cycles/pixel.

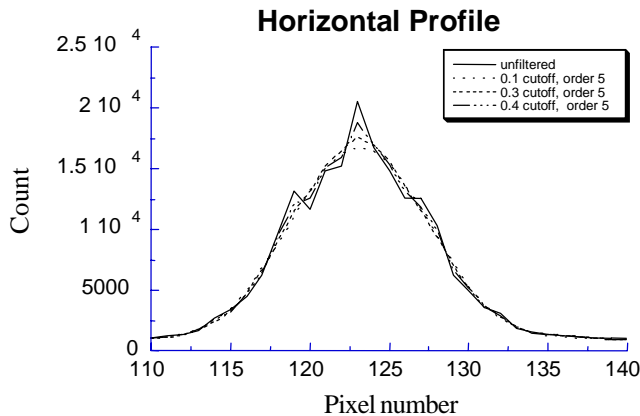


**Fig. 6** Horizontal profiles through the center of the leftmost sphere (i.e., the 1.6 cm sphere) in Figures 5(a), (b), (d) and (e).

pixel substantially reduce the hole-pattern; however, the processed image shows poorer spatial resolution as demonstrated in Figures 5(b) and 6.

At cutoff frequencies of 0.4-0.5 cycles/pixel, the processed images show good spatial resolution, but the hole-pattern artifact remains as seen in Figure 5(e) and 5(f). With cutoff frequencies of 0.2-0.3 cycles/pixel, the hole-pattern is reduced with minimal degradation of spatial resolution, as shown in Figure 5(c) and 5(d). Figure 6 shows graphically how the filter function reduces the hole-pattern with minimal degradation of the spatial resolution. This agrees with arguments made about the transfer function in Section IIC.

### C. SPECT Images of Phantom

In Figures 7 and 8, we compare the SPECT reconstructed images of the phantom containing 3 hot spheres obtained using the FBP and OS-EM algorithms without any compensation and the OS-EM algorithm with approximate compensation of the CDRF of the ME collimator by modeling the geometric component of the CDRF. The results show that the hole-pattern ar-

tifact was not seen for the 64 x 64 matrix size as shown in Figure 7. The hole-pattern artifact is seen in the 128 x 128 reconstructed images for FBP and the OS-EM algorithm without any compensation as shown in Figure 8. However, images reconstructed with OS-EM and an appropriate compensation of the distance-dependent CDRF show significant improvement in resolution and no hole-pattern artifact.

## IV. DISCUSSION AND CONCLUSION

The measurements of the PRF of a GE ME collimator with  $^{67}\text{Ga}$  demonstrated that it is dependent on a source distance. The hole-pattern artifact is also seen at all distances and  $^{67}\text{Ga}$  photon energies for images with small pixel size. For planar imaging, we demonstrated that a filter function could be designed to dramatically reduce the hole-pattern artifact with minimal resolution degradation. However, the filter requires that the distance between the tumor and the collimator must be known. In clinical practice, the distance can only be estimated.

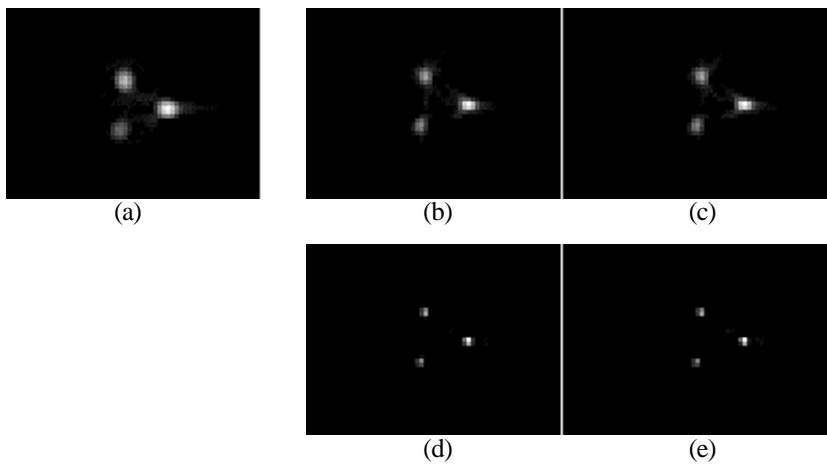


**Fig. 7** The 64x64 matrix size reconstructed images obtained using (a) the conventional filtered backprojection algorithm, the OS-EM algorithm without the CDRF compensation after (b) 2 and (c) 5 iterations and the OS-EM algorithm with the CDRF compensation after (d) 2 and (e) 5 iterations.

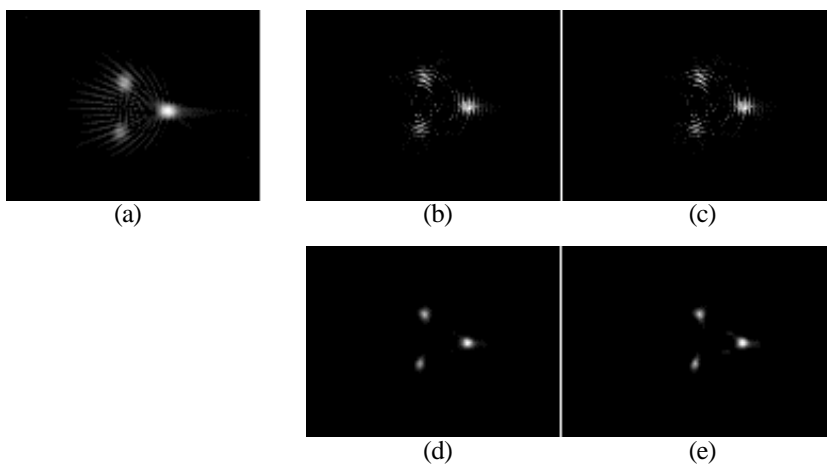


**Fig. 8** The 128x128 matrix size reconstructed images obtained using (a) the conventional filtered backprojection algorithm, the OS-EM algorithm without CDRF compensation after (b) 2 and (c) 5 iterations and the OS-EM algorithm with CDRF compensation after (d) 2 and (e) 5 iterations.

In SPECT imaging, the hole-pattern artifact is not seen in reconstructed images with large pixels. For reconstructed images with small pixels and without any compensation using the FBP or the OS-EM algorithm show hole-pattern artifact. With an appropriate CDRF compensation, we

found a substantial reduction in reconstructed image artifacts and an improvement in image resolution when using the OS-EM algorithm.

In conclusion, in  $^{67}\text{Ga}$  images it is feasible to improve image quality by appropriate

filtering of the planar images and by compensating for the CDRF of the ME collimator used in SPECT imaging. The method is efficient and allows for the incorporation of the spatially varying in the projection and backprojection steps of an iterative OS-EM algorithm. Even though only the average geometric response function is used, substantial improvements are seen in the reconstructed images.

### **Acknowledgments**

The work was supported by a Fellowship Grant from Thai government for C. Tocharoenchai and the US Public Health Grant CA 39463. The contents of this work are solely the responsibility of its authors and do not necessarily represent the official views of the Public Health Service. The authors would like to thank the staff of the Nuclear Medicine Division, Department of Radiology, the University of North Carolina Hospital, NC for their help and cooperation. Our thanks go to Daniel E. Wessell for his help in editing this manuscript.

### **REFERENCES**

1. Leichner PK, et al. SPECT Imaging of Fluorine-18. *J Nucl Med* 1995;36:1472-5
2. Zeng GL, et al. Iterative Reconstruction of Fluorine-18 SPECT Using Geometric Point Response Correction. *J Nucl Med* 1998;39:124-30
3. Zeng GL and Gullberg GT. Frequency Domain Implementation of the Three-Dimensional Geometric Point Response Function Correction in SPECT Imaging. *IEEE Nucl Sci Symp and Med Imag Conf*, Santa Fe, NM, 1991:1943-7
4. Hudson HM and Larkin RS. Accelerated image reconstruction using ordered subsets of projection data. *IEEE Trans Med Im* 1994;13:601-9
5. Lalush DS, Karimi S and Tsui BMW. Convergence and resolution recovery of block iterative EM algorithms modeling 3D detector response in SPECT. *IEEE Nucl Sci Symp Conf Rec*, Anaheim, California, 1996
6. Weber DA, et al. MIRD: Radionuclide Data and Decay Schemes. New York: The Society of Nuclear Medicine, Inc., 1989, pp.84-84
7. Metz CE, Atkins FB and Beck RN. The Geometric Transfer Function Component for Scintillation Camera Collimators with Straight Parallel Holes. *Phys Med Biol* 1980;25:1059-70
8. Frey EC, Ju ZW and B.M.W. Tsui BMW. A Fast Projector-Backprojector Pair Modeling the Asymmetric, Spatially Varying Scatter Response Function for Scatter Compensation in SPECT Imaging. *IEEE Trans Nucl Sci* 1993;40:1192-7